

Plasma electron temperature measurement by foil soft-X-Ray spectrometer installed on TUMAN-3M and Globus-M2 tokamaks

© A.V. Voronin,¹ V.Yu. Goryainov,^{1,2} V.V. Zabrodsky,¹ E.V. Sherstnev,¹ V.A. Kornev,¹ P.N. Aruev,¹
G.S. Kurskiy,¹ N.A. Zhubr,¹ A.S. Tukachinsky¹

¹ Ioffe Institute,
195251 St. Petersburg, Russia

² Peter the Great Saint-Petersburg Polytechnic University,
195251 St. Petersburg, Russia
e-mail: vgoryainov@mail.ioffe.ru

Received June 18, 2021

Revised August 12, 2021

Accepted August 24, 2021

Technical solution were presented for a foil spectrometer installed on the Globus-M2 and TUMAN-3M tokamaks for measuring the electron plasma temperature. Measurements have been carried out of the time dependence of the plasma temperature in the central region of tokamaks. Using of integrated photodetectors and unique beryllium foils with a thickness of 14–80 μm made it possible to increase the sensitivity of the spectrometer. An important quality of the foils used were the increased values of strength, plasticity, homogeneity, and the absence of surface and internal defects. The combined use of the spectrometer with Thomson scattering diagnostics made it possible to carry out regular temperature measurements in the Globus-M2 tokamak with a high spatial and temporal resolution. The influence of impurities is estimated on the measurement of the electron temperature of the plasma.

Keywords: foil spectrometry, tokamak, plasma, continuum, bremsstrahlung, electron temperature, soft-X-Ray, Si-photodiode.

DOI: 10.21883/TP.2022.15.55263.188-21

Introduction

Diagnostic methods based on the measurement of spectrum and intensity of X-ray emission are successfully used in the study of plasma. In combination with other methods of studies, the X-ray diagnostics is quite useful for studying various processes in the tokamak plasma. For example, it allows to study internal MHD-oscillations of plasma and to determine location of the surfaces with a rational value of safety factor q [1,2], to evaluate electron losses by using the electron-cyclotron emission ECE [3] and runaway electrons RE [4], Edge Localised Modes ELMs [5,6], to monitor L–H transition [7] and many more [8–16]. Such devices are widely used in the tokamaks JET [17], MAST [8], DIII-D [18], Asdex-Upgrade [19], PDX [20], NSTX [21–23], EAST [5], MST [24], TCV [25,26], COMPASS [27,28]. The measurement in X-ray devices is performed without interaction into the process under study.

Equipment for temperature registration is one of the most demanded for the study of the laboratory plasma behavior. Today, the electron temperature is determined by the value of plasma conductivity, own emission of intensity of the linear and solid spectrum of plasma, as well as electron-cyclotron frequency and its harmonics [29–31].

Herein, we presented a technical solution for a foil X-ray multichannel spectrometer installed at the Globus-M2 and TUMAN-3M tokamaks for the determination of the electron temperature of plasma on the plasma column axis with a high time resolution.

In the spherical Globus-M2 tokamak (minor radius $a = 0.24$ m, major radius $R = 0.36$ m, magnetic field on the torus axis $B_T = 0.5–0.9$ T, plasma current $I_p = 150–400$ kA) [32], two intercomplementary diagnostics were used for the measurement of the electron component of plasma temperature — Thomson scattering of the laser beam during its interaction with plasma [33] and foil spectrometry of soft X-ray emission. By means of a laser with the pulses frequency of 300 Hz the temperature was registered in 10 spatial regions of plasma column during the tokamak discharge. High cost and limited operation time of the laser did not allow to use that diagnostics all the time. The developed foil spectrometer, in addition to the measurement passivity, features a low cost, small dimensions, and simple operation versus Thomson scattering diagnostic.

The foil spectrometer provided continuous temperature measurement with the discretization frequency of ~ 50 kHz and applied during the whole experimental campaign. At that, the real spectrometer frequency as a part of the Globus-M tokamak was 30 kHz. It was limited by the transmission band of the optic coupler built into the tokamak data acquisition system. Main disadvantage of that diagnostics is a high error of calculation of the electron temperature. However, it was far more cheaper than the Thomson scattering diagnostics. An assumption of the Maxwell distribution of electrons by energies is required for the performance of the measurements of electron temperature of hydrogen/deuterium plasma. The plasma purity and the

value of electron temperature of $T_e > 100$ eV are needed as well.

In the TUMAN-3M tokamak ($a = 0.22$ m, $R = 0.53$ m, $B_T = 1.0$ T, $I_P = 190$ kA) [34] the measurement of the electron temperature was performed by means of two foil spectrometers. They differed from each other by location in the tokamak, sensitivity, action time, and design. Sensors and foils of main spectrometer (total of 9 chords) installed earlier onto the tokamak were in inert gas and connected to the vacuum chamber via beryllium foil with the thickness of $50 \mu\text{m}$. Sensors with pre-amplifiers and thin foils of another spectrometer developed today were located inside the vacuum chamber of the tokamak and had higher time resolution than the sensors of the main spectrometer. The electron temperature measured by the developed spectrometer was compared with the measurements of the temperature by the main spectrometer.

1. Foil spectrometer

In hydrogen/deuterium plasma free from impurities at the electron temperature above 100 eV bremsstrahlung X-ray radiation occurring due to the acceleration of electrons in the Coulomb field of ions plays the main role versus recombination, linear and cyclotron emissions [35]. Spectral power density of bremsstrahlung per the plasma volume unit dV subject to Maxwell distribution of electrons by energies can be described by the formula [13,36]:

$$\frac{dP_{ff}}{d\nu \cdot dV} \approx 10^{-28} \cdot Z_{\text{eff}}^2 \cdot \langle g_{ff} \rangle \cdot n_i \cdot n_e \cdot \sqrt{\frac{\chi_H}{T_e}} \cdot \exp\left(-\frac{h\nu}{T_e}\right), \tag{1}$$

where χ_H is the hydrogen ionization potential, T_e is the temperature of electrons, [eV], n_i and n_e are densities of ions and electrons, accordingly, [cm^{-3}], h is the Plank's constant, ν is the frequency of photons, Z_{eff} is the effective charge of plasma, $\langle g_{ff} \rangle$ is the Gaunt-factor averaged by energies for the free-free transitions, which can be calculated in accordance with [37]. If the photon energy $\varepsilon = h \cdot \nu$, then the intensity of bremsstrahlung can be represented as

$$I_{ff} \propto f(T_e, n_e, Z_{\text{eff}}) \cdot \exp\left(-\frac{\varepsilon}{T_e}\right). \tag{2}$$

Here, f is the function depending on the electron temperature, density, effective charge and Gaunt-factor; the photon energy ε is expressed in eV. If this radiation falls onto a diode with foil of a determined thickness, then the signal from the detector can be represented as

$$i(t) \propto f(T_e, n_e, Z_{\text{eff}}) \cdot \int_0^\infty F^{FPU}(\varepsilon) \cdot F^{foil}(\varepsilon) \cdot \exp\left(-\frac{\varepsilon}{T_e}\right) d\varepsilon, \tag{3}$$

where F^{FPU} and F^{foil} are spectral characteristics of the diode and filter, accordingly.

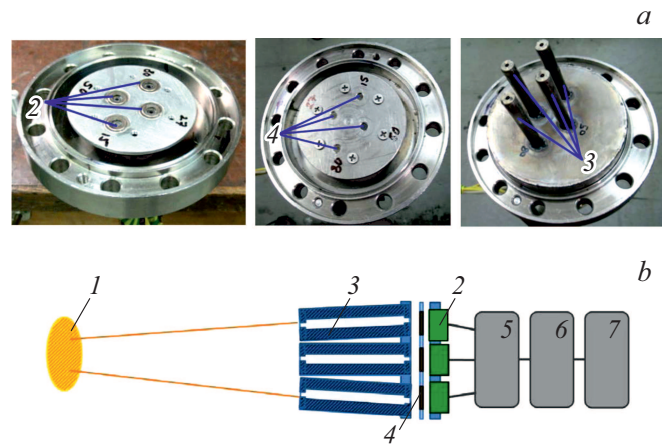


Figure 1. *a* — elements of four-channel spectrometer installed on the vacuum flange, from the left to the right: detectors, foils and collimators; *b* — diagram of foil spectrometer: 1 — plasma, 2 — photodiodes with integrated amplifiers, 3 — collimators, 4 — beryllium foils, 5 — stabilized power source, 6 — analog-to-digital converter, 7 — computer.

When using two detectors with foils of various thickness that receive the X-ray radiation from the same region, the electron temperature can be determined based on the ratio

$$\frac{i_1}{i_2} = R(T_e) = A \cdot \frac{\int_0^\infty F^{FPU}(\varepsilon) \cdot F_1^{foil}(\varepsilon) \exp\left(-\frac{\varepsilon}{T_e}\right) d\varepsilon}{\int_0^\infty F^{FPU}(\varepsilon) \cdot F_2^{foil}(\varepsilon) \exp\left(-\frac{\varepsilon}{T_e}\right) d\varepsilon}, \tag{4}$$

where A is the coefficient that considers the difference of sensors registration channels, which was determined as a result of the instrument calibration by the reference radiation source. Indices 1 and 2 correspond to various-thick foils of detectors. Integration by the photon energy was performed by the region of detector sensitivity 10 eV–50 keV.

Based on the known function $R(T_e)$ and amplitudes of signals from the detectors, we can obtain the value of temperature for every moment of time. By changing the foils thickness, we can vary the instrument sensitivity to different ranges of temperatures. Use of several channels (more than two) with different foil thicknesses allowed to select the operational range of the spectrum without presence of impurities radiation. For this purpose, herein we presented four-channel and three-channel spectrometers for the Globus-M2 and TUMAN-3M tokamaks, accordingly, which allowed to perform the measurement of the temperature of plasma in the central range of the plasma column with the time resolution of $\sim 20 \mu\text{s}$. The results of measurements of alternative diagnostics provided additional calibration and verification of these measurements.

The developed spectrometer consisted of detectors, beryllium foils, collimators, and a stabilized source of power. Overview of the flange equipped with detectors, filters and collimators, as well as the diagram of spectrometer are given in Fig. 1. All elements of the instrument were

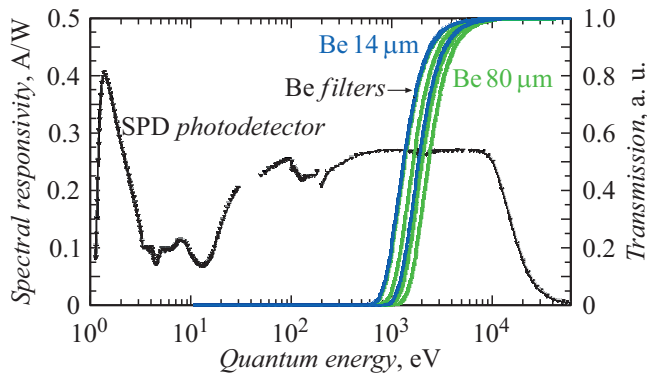


Figure 2. The spectrum characteristic of the SPD photodiode and transmission of beryllium foils of various thickness.

Main parameters of the detector

Amplification	10^7 V/A
Noise voltage	< 10 mV
Diameter of active area	3.2 mm
Signal-to-noise ratio	~ 100
Rise time	< 20 μ s

mounted on the DN80 flange on the face oriented into the vacuum chamber of the tokamak. Collimators with the length of 60 mm and the inlet hole diameter of 3 mm collected radiation from plasma in the equatorial region of the tokamak along the observation line with a low steradian.

Collimators alignment was performed within the visible region of spectrum by means of LEDs installed instead of the detectors and foils. Images of beams from LEDs were formed on the screen in the region of their crossing with it; the screen is located at a distance corresponding to that from detectors to the center of plasma column (970 mm for the Globus-M2 and 580 mm for the TUMAN-3M). Superposition of images was performed by mechanical bending of collimators. The spot image diameter was ~ 20 mm.

Detectors were made by Technoexan CJSC specially for that spectrometer [38]. In the applicable SPD detectors (silicon precision detector) [39,40] a thin enough „dead layer“ was formed that allowed to obtain a high output signal. Transimpedance amplifier was connected to each detector. The main peculiarity of the developed detectors referred to their high sensitivity and time resolution, which allowed to register fast processes occurring in the tokamak plasma. Spectral characteristic $F^{FPU}(\epsilon)$ of the detectors is given in Fig. 2 [40]. Table below contains main electrical and dynamical characteristics of the detector.

Power supply and signals from detectors are connected through vacuum connectors located on the flange. The power source provided the output voltage of ± 5 V.

Beryllium foils were manufactured in Institute of Machinery, Materials, and Transport of the Peter the Great Polytechnic University [41,42] by multipass hot cross rolling.

An important feature of these foils (with the minimum possible thickness of $5 \mu\text{m}$) referred to high values of strength, plasticity, homogeneity, absence of superficial and internal defects. Foil thicknesses on the photodetectors of the spectrometer in Globus-M2 tokamak, were 15, 27, 50 and $80 \mu\text{m}$. On the TUMAN-3M tokamak— 27, 14 and $40 \mu\text{m}$. Spectral characteristics of foils F^{foil} were calculated by using the database [43]. They are shown in Fig. 2 on the right.

Calibration of the spectrometer channels was performed by using the red LED radiation at the wavelength of 1050 nm. Beryllium foils were absent during calibration. A collar with LED was installed on to each of four collimators one by one. The measurement of voltage was performed at the detector output of each channel. Subject to these measurements the coefficient A was determined, which is required for the calculation of dependence of the ratio of sensor signals $R(T_e)$ on the temperature. Results of calculations for the Globus-M2 tokamak are given in Fig. 3. As we can see, the highest sensitivity $R(T_e)$ to the temperature was manifested when we selected the pairs of foils with the least and the highest thicknesses, in the manner that the second signal differs from noise.

The process of determination of the dependence of temperature on the time $T_e(t)$ referred to the comparison of the calculation function of the ratio of signal to the temperature $R(T_e)$ with experimental dependence of the signals ratio on the time $R(t)$. This process was performed by means of an algorithm built-into the Combiscope software developed for the collection and processing of data of the Globus-M2 tokamak. Similar software was used at the TUMAN-3M tokamak.

Disposition of diagnostics and four-channel spectrometer installed at the Globus-M2 tokamak is shown in Fig. 4, *a*.

Four-channel spectrometer was placed on duct above the equatorial plane of the tokamak, this is why collimators were inclined to the equator at the angle of $8^\circ 41'$ for the

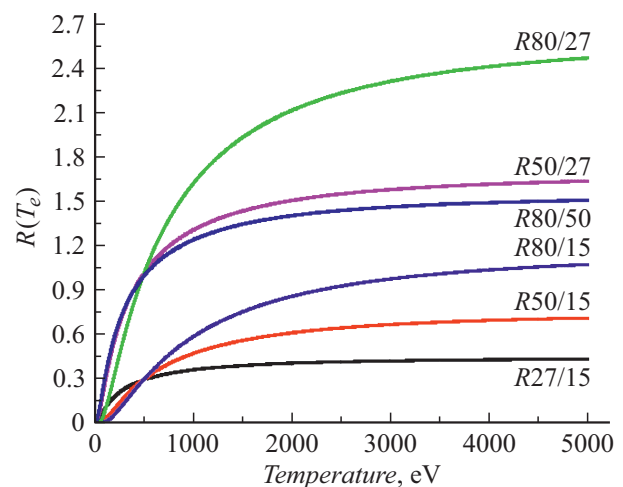


Figure 3. Dependences on $R(T_e)$ for various thicknesses (15, 27, 50, $80 \mu\text{m}$) of foils applicable at the Globus-M2 tokamak subject to the calibration coefficient A .

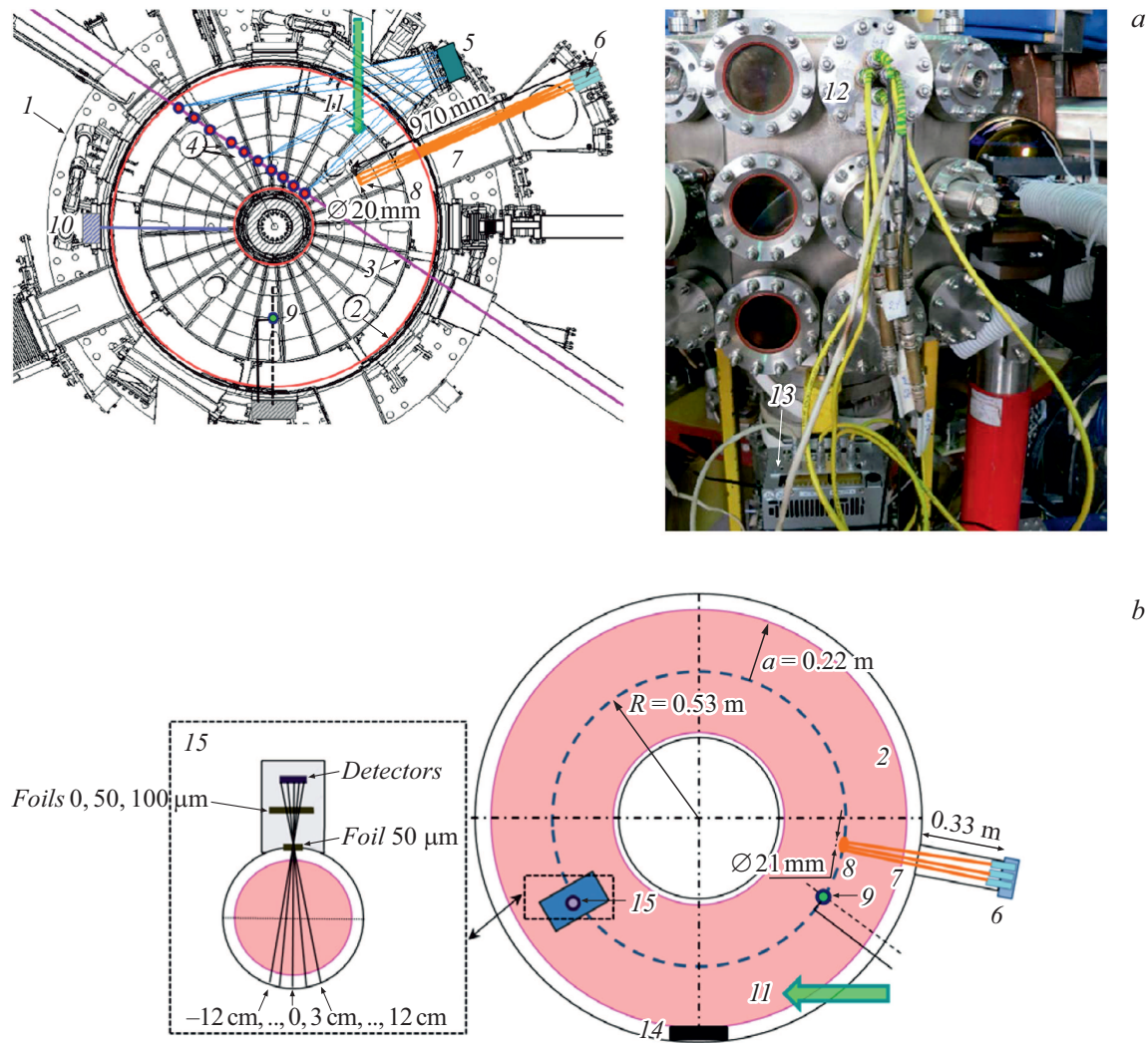


Figure 4. *a* — location of diagnostics and four-channel spectrometer installed at the Globus-M2 tokamak: 1 — cross-section of chamber in the equatorial plane, 2 — external boundary of plasma, 3 — probing laser beam, 4 — regions of the temperature measurement by laser, 5 — objective, 6–8 — collimators, boundaries of the radiation collection and the region of the spectrometer temperature measurement, 9 — regions of measurement of the middle-chord density by microwave interferometer, 10 — photodetectors for the measurement of radiation of CIII line, 11 — location and direction of neutral injection NBI, 12, 13 — flange and power source of the spectrometer; *b* — diagram of equatorial cross-section of the TUMAN-3M tokamak: 14 — limiter, 15 — location and diagram of the main spectrometer.

collection of the plasma radiation from the central region of the vacuum chamber. Collimators were also inclined relative to each other for the collection of radiation from the same region with the diameter of 20 mm at the distance of 970 mm from the detectors (position 8 in Fig. 4, *a*).

By means of the Thomson scattering diagnostics we performed the measurement of temperature in 10 spatial regions of the plasma column (position 4 in Fig. 4, *a*) up to 35 times during the tokamak discharge. Duration of the probing laser pulse was ~ 10 –50 ns, the interval between pulses was ~ 2.5 –3 ms. Laser beam passed in the equatorial plane near to tokamak central column; the scattered radiation collection system was also located in the equatorial plane.

Diagram of the TUMAN-3M tokamak's equatorial cross-section with diagnostics is shown in Fig. 4, *b*. The

developed three-channel spectrometer was located in the equatorial plane. The diagram of the main X-ray diagnostics (position 15) is shown close-up, whose temperature measurements were performed together with the comparison of the results to that obtained by using the three-channel spectrometer.

2. Results

Fig. 5 shows the evolution of the discharge parameters of the deuterium plasma at the TUMAN-3M tokamak with neutral hydrogen injection of various duration and power of the beam. Digit 1 refers to electron temperature measured in radial direction of the torus by means of the developed three-channel spectrometer with the foil thicknesses of 14

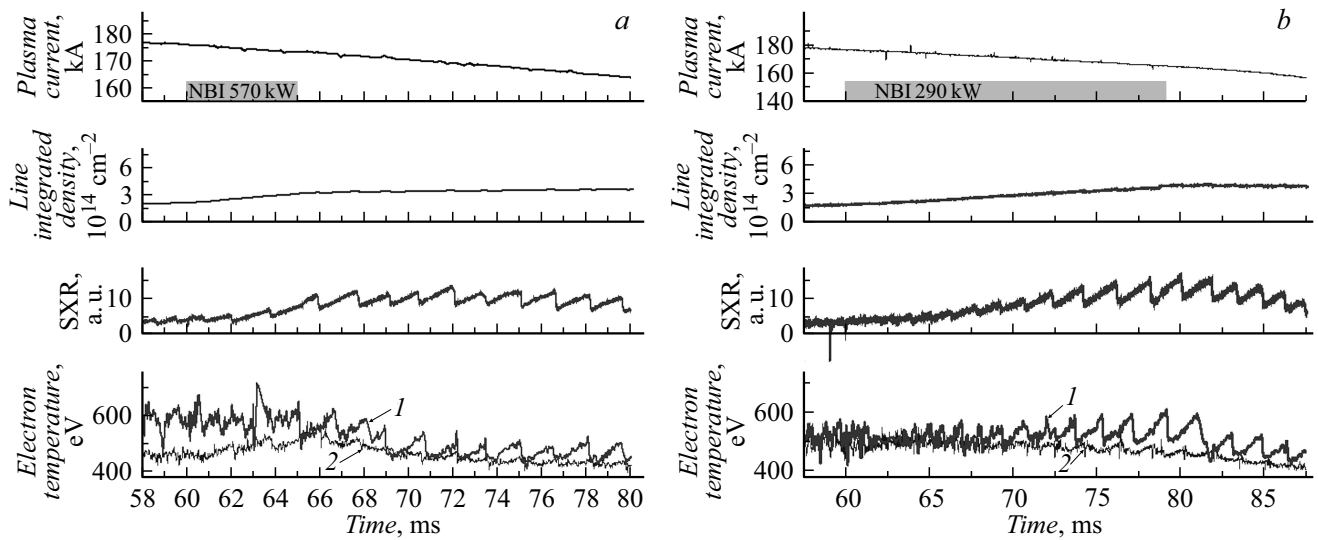


Figure 5. Evolutions of the parameters of discharges #19022017 (*a*) and #19022014 (*b*) in the TUMAN-3M tokamak. 1 — electron of plasma obtained by spectrometer with the 14 and 27 μm -thick foils, 2 — the same for the 100 and 150 μm -thick foils.

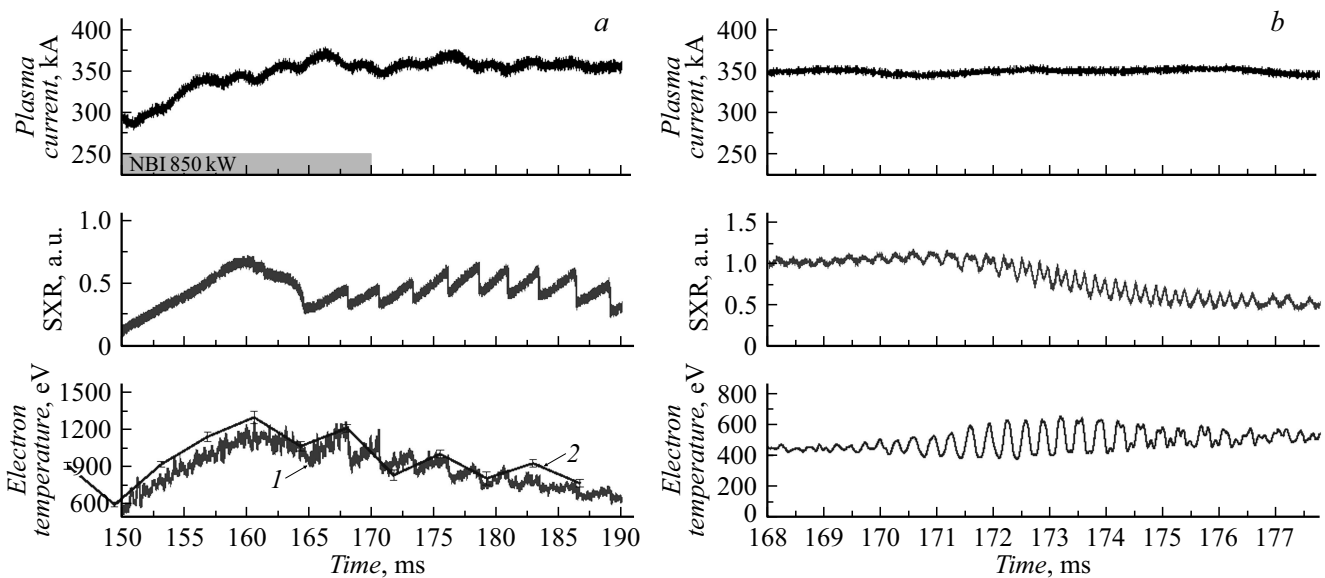


Figure 6. Evolution of parameters of plasma discharges in the Globus-M2 tokamak. *a* — discharge with sawtooth oscillations, #38835; *b* — discharge with mod excitation of the „snake“ type, #38838. Electron temperature of plasma obtained by means of 1 — foil spectrometer, 2 — the Thomson scattering diagnostics.

and 27 μm . Line 2 is the temperature obtained by the main spectrometer with the foil thicknesses of 100 and 150 μm . It can be seen that during beam injection the measured temperatures match, when the medium-chord density of plasma exceeded $3 \cdot 10^{14} \text{ cm}^{-2}$. Temperature decrease was observed after the end of injection on both diagnostics. The values obtained by means of a pair of foils with the thickness of 40, 27 and 40, 14 μm , on the three-channel spectrometer appeared to be underestimated, which could be associated with the effect of impurities of stainless steel [15], which the tokamak limiter is made of. It can be seen that the three-channel foil spectrometer provided the

temperature measurement at a higher time resolution versus the resolution obtained by means of the main spectrometer.

Example of capabilities of the main foil spectrometer at the Globus-M2 tokamak is demonstrated in Fig. 6, where the processes are shown in various time scales.

Fig. 6, *a* shows discharge parameters with sawtooth oscillations. Measurement of the electron temperature in plasma was performed simultaneously by means of foil spectrometer and the Thomson scattering diagnostics. The maximum temperature of radial profile measured by the Thomson scattering diagnostics was at the central chord, which is the closest in the poloidal projection to

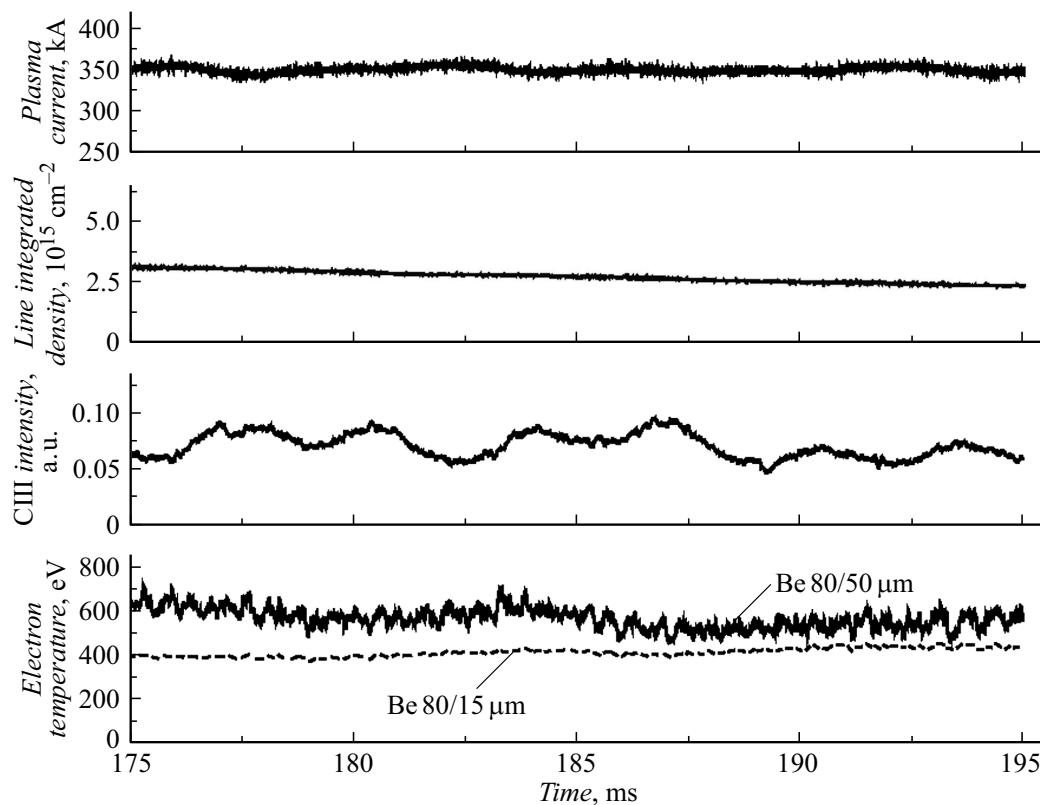


Figure 7. Parameters of the discharge #38837 of the Globus-M2 tokamak.

the spectrometer measurement region. In both cases, the two diagnostics registered temperature oscillations on the plasma column axis with the specific frequency of ~ 300 Hz. However, the foil spectrometer provided the temperature measurement at a higher time resolution versus the resolution measured by the Thomson scattering diagnostics. Fig. 6, *b* presents the parameters of Ohmic discharge caused by the mod excitation of the „snake“ type. It can be seen that the foil spectrometer registered oscillations of the electron temperature at the specific frequency of ~ 30 kHz.

Non-conformance of the results of measurements of the electron temperature, obtained by the spectrometer with different thicknesses of foils, to the Thomson scattering diagnostics could be caused by the effect of radiation of hydrogen impurities, since the primary wall of the Globus-M2 tokamak was coated with graphite tiles. Fig. 7 shows parameters of the ohmic discharge with a moderate number of carbon in plasma. The lower graph shows values of electron temperature measured by spectrometer with pairs of beryllium foils of various thicknesses. The instrument error in the measurement did not exceed 20%. It can be seen that the measured temperature has considerably risen with the increase of the foil thickness. It can be assumed that the effect of carbon radiation has fallen as far as the foil thickness was increased, and the measured temperature tended to the true one.

Conclusion

The foil spectrometer for the measurement of the plasma electron temperature in the Globus-M2 and TUMAN-3M tokamaks was developed, manufactured and tested. Application of photodetectors with the integrated amplifiers and unique thin beryllium foils allowed to increase the sensitivity and quick action of the spectrometer. The algorithm was prepared for the calculation of the temperature dependence on time by measured signals of soft X-ray radiation. Measurements were performed of the dependence of the plasma electron temperature on time in the central region of the tokamaks. The measured temperatures mainly agree with that obtained by means of alternative diagnostics. Joint use of the foil spectrometer with the Thomson scattering diagnostics allowed to perform regular measurements of the temperature in the Globus-M2 tokamak with high spatial and time resolutions. Comparison of the results at the TUMAN-3M tokamak has shown the applicability of the method for beryllium foils with the thickness below $100 \mu\text{m}$. Assessment was performed as to the effect of impurities for the measurement of the plasma electron temperature by using the foil spectrometer.

Acknowledgements

The development of the foil spectrometer was funded under the state assignment of Ioffe Institute 0040-2019-

0023. Experiments were performed on the Unique Scientific Facility „Spherical tokamak Globus-M“, which is incorporated in the Federal Joint Research Center „Material science and characterization in advanced technology“ at the Ioffe Institute as well as the TUMAN-3M tokamak USF. This work was supported by the Ministry of science and higher education of Russian Federation in the framework of the state contract in the field of science under project № 0784-2020-0020.

Conflict of interest

The authors declare that they have no conflict of interest.

References

- [1] L. Xu, L. Hu, K. Chen, E. Li, F. Wang, M. Xu, Y. Duan, T. Shi, J. Zhang, R. Zhou, Y. Chen. *Phys. Plasmas*, **19**, 122504 (2012).
- [2] S. Mirnov. *Physical Processes in Tokamak Plasma* (Atomizdat, Moscow, 1983), p. 116.
- [3] H. Lu, J. Luo, F. Zhong, X. Zha, L. Hu. *Eur. Phys. J. D*, **66**, 213 (2012).
- [4] A. Tukachinsky, L. Askinazi, I. Balachenkov, A. Belokurov, D. Gin, N. Zhubr, V. Kornev, S. Lebedev, E. Khil'kevich, I. Chugunov, A. Shevelev. *Tech. Phys. Lett.*, **42** (12), 1167 (2016).
- [5] K. Chen, L. Xu, L. Hu, Y. Duan, X. Li, Y. Yuan, S. Mao, X. Sheng, J. Zhao. *Rev. Sci. Instrum.*, **87**, 063504 (2016).
- [6] Y. Li, G. Xu, K. Tritz, X. Lin, H. Liu, Y. Chen, S. Li, F. Yang, Z. Wu, L. Wang, H. Lan, X. Li, W. Zhang, G. Hu. *Fusion Eng. Des.*, **137**, 414 (2018).
- [7] L. Askinazi, V. Kornev, S. Krikunov, L. Krupnik, S. Lebedev, A. Smirnov, M. Tendler, A. Tukachinsky, M. Vildjunas, N. Zhubr. *J. Phys.: Conf. Ser.* **123**, 012010 (2008).
- [8] M. Cecconello, O. Jones, L. Garzotti, K. McClements, M. Carr, S. Henderson, S. Sharapov, I. Klimek and the MAST Team. *Nucl. Fusion*, **55**, 032002 (2015).
- [9] T. Onchi, R. Ikezoe, K. Oki, A. Sanpei, H. Himura, S. Masamune. *Rev. Sci. Instrum.*, **81**, 073502 (2010).
- [10] L. Askinazi, M. Vild'zhunas, V. Golant, V. Kornev, S. Krikunov, S. Lebedev, G. Razdobarin, V. Rozhdestvensky, E. Shevkin, A. Tukachinsky, S. Tsaun, N. Zhubr. *29th EPS Conference on Plasma Phys. and Contr. Fusion, Montreux, 17–21 June 2002 ECA*, vol. 26B, P-2.070 (2002).
- [11] M. Kantor, A. Altukhov, V. Belik, L. Esipov, D. Kouprienko L. Shmaenok, V. Yermolayev. *30th EPS Conference on Contr. Fusion and Plasma Phys., St. Petersburg, 7–11 July 2003 ECA*, vol. 27, A P-2.60 (2003).
- [15] S. von Goeler, W. Stodiek, H. Eubank, H. Fishman, S. Grebenshchikov, E. Hinnov. *Nucl. Fus.*, **15** (2), 301 (1975).
- [13] Huddleston R and Leonard S. *Plasma Diagnostic Techniques* (Academic Press, NY.–London, 1965), p. 304.
- [14] V. Andreev, I. Bragin. *Plasma Diagnostics with Conductivity Probes* (St.-Petersburg: SUAI 2000), p. 4.
- [15] K. Nishimura, A. Sanpei, H. Tanaka, G. Ishii, R. Kodera, R. Ueba, H. Himura, S. Masamune, S. Ohdachi, N. Mizuguchi. *Rev. Sci. Instrum.*, **85**, 033502 (2014).
- [16] L. Delgado-Aparicio, J. Wallace, H. Yamazaki, P. VanMeter, L. Reusch, M. Nornberg, A. Almagari, J. Maddox, B. Luethi, M. Rissi, T. Donath, D. Den Hartog, J. Sarff, P. Weix, J. Goetz, N. Pablant, K. Hill, B. Stratton, P. Efthimion, Y. Takase, A. Ejiri. *M. Rev. Sci. Instrum.*, **89** (10), 10G116 (2018). DOI: 10.1063/1.5038798
- [17] B. Alper, S. Dillon, A. Edwards, R. Gill, R. Robins, D. Wilson. *Rev. Sci. Instrum.*, **68** (1), 778 (1997).
- [18] E. Hollmann, L. Chousal, R. Fisher, R. Hernandez, G. Jackson, M. Lanctot, S. Pidcoe, J. Shankara, D. Taussig. *Rev. Sci. Instrum.*, **82** (11), 113507 (2011).
- [19] V. Igochine, A. Gude, M. Maraschek, ASDEX Upgrade team. IPP report, 1/338 Mai, 2010.
- [20] E. Silver, M. Bitter, K. Brau, D. Eames, A. Greenberger, K. Hill, D. Meade, W. Roney, N. Sauthoff, S. Von Goeler. *Rev. Sci. Instrum.*, **53**, 1198 (1982).
- [21] L. Delgado-Aparicio, D. Stutman, K. Tritz, M. Finkenthal, R. Bell, D. Gates, R. Kaita, B. LeBlanc, R. Maingi, H. Yuh, F. Levinton, W. Heidbrink. *Plasma Phys. Control. Fusion.*, **49** 1245 (2007).
- [22] B. LeBlanc, R. Bell, S. Kaye, D. Stutman, M. Bell, M. Bitter, C. Bourdelle, D. Gates, R. Maingi, S. Medley, J. Menard, D. Mueller, S. Paul, A. Roquemore, A. Rosenberg, S. Sabbagh, V. Soukhanovskii, E. Synakowski, J. Wilson and the NSTX Research Team. *Nucl. Fusion*, **44**, 513 (2004).
- [23] B. Stratton, M. Biter, K. Hill, D. Hillis, J. Hogan, *Passive Spectroscopic Diagnostics for Magnetically-Confined Fusion Plasmas*. (United States: N. p., 2007). DOI: 10.2172/962715
- [24] M. McGarry, P. Franz, D. Den Hartog, J. Goetz. *Plasma Phys. Control. Fusion.*, **56**, 125018 (2014).
- [25] I. Furno. *Fast Transient Transport Phenomena Measured by soft X-ray Emission in TCV Tokamak Plasmas*. LRP 703/01, August 2001.
- [26] M. Anton, H. Weisen, M. Dutch, W von der Linden, F. Buhlmann, R. Chavan, B. Marletaz, P. Marmillod, P. Paris. *Plasma Phys. Controlled Fusion.*, **38**, 1849 (1996).
- [27] M. Im išek, J. Mlynář, V. Löffelman, V. Weinzettl, T. Odstrčil, M. Odstrčil, M. Tomeš. *Nukleonika*, **61** (4), 403-8 (2016).
- [28] M. Imříšek, V. Weinzettl, J. Mlynář, T. Odstrčil, M. Odstrčil, O. Ficker, J. Pinzon, C. Ehrlacher, R. Panek, M. Hron. *Rev. Sci. Instrum.*, **85**, 11E433 (2014).
- [29] Podgorny M., *Plasma Diagnostic Lectures* (Atomizdat, M., 1968), p. 88.
- [30] Zh. Qiuping, Ch. Cheng, M. Yuedong. *Plasma Sci. Technol.*, **11** (5), 560 (2009).
- [31] V. Timokhin, A. Rykachevskii, I. Miroshnikov, V. Sergeev, M. Kochergin, A. Koval', E.E. Mukhin, S. Tolstyakov, A. Voronin. *Tech. Phys. Lett.*, **42** (8), 775 (2016).
- [32] V. Minaev, V. Gusev, N. Sakharov, V. Varfolomeev, N. Bakharev, V. Belyakov, E. Bondarchuk, P. Brunkov, F. Chernyshev, V. Davydenko, V. Dyachenko, A. Kavin, S. Khitrov, N. Khromov, E. Kiselev, A. Kononov, V. Kornev, G. Kurskiev, A. Labusov, A. Melnik, A. Mineev, M. Mironov, I. Miroshnikov, M. Patrov, Yu. Petrov, V. Rozhansky, A. Saveliev, I. Senichenkov, P. Shchegolev, O. Shcherbinin, I. Shikhovtsev, A. Sladkomedova, V. Solokha, V. Tanchuk, A. Telnova, V. Tokarev, S. Tolstyakov, E. Zhilin. *Nucl. Fusion.*, **57**, 066047 (2017).

- [33] G. Kurskiev, S. Tolstyakov, A. Berezutskiy, V. Gusev, M. Kochergin, V. Minaev, E. Mukhin, M. Patrov, Yu. Petrov, N. Sakharov, V. Semenov, P. Chernakov. *Thermonucl. Fusion.*, **2**, 81 (2012).
- [34] S. Lebedev, M. Andrejko, L. Askinazi, V. Golant, V. Kornev, L. Levin, V. Rozhansky, M. Tendler, A. Tukachinsky. *Plasma Phys. Control. Fusion.*, **36**, B289 (1994).
- [35] F. Scholze, R. Klein, R. Müller. *Metrologia*, **43**, 6 (2006).
- [36] S. Luk'yanov. *Hot Plasma and Controlled Nuclear Fusion* (Nauka, M., 1975), p. 154.
- [37] W. Karzas, R. Latter. *Astrophysical J. Suppl. Ser.*, **6**, 167 (1960).
- [38] Electronic source. Available at:
<http://technoexan.ru/en/products/sildet.php>
- [39] P. Aruev, Yu. Kolokolnikov, N. Kovalenko, A. Legkodymov, V. Lyakh, A. Nikolenko, V. Pindyurin, V. Sukhanov, V. Zabrodsky. *Nucl. Instrum. Meth. Phys. Res. A*, **603**, 58 (2009).
- [40] P. Aruev, S. Bobashev, A. Krassilchtchikov, A. Nikolaev, D. Petrov, E. Sherstnev. *Instrumen. Experimental Techniq.*, **64**, 93 (2021). DOI: 10.1134/S0020441220060147
- [41] V. Mishin, I. Shishov, A. Minchena. *Mater. Phys. Mechan.*, **38** (1), 40 (2018).
- [42] V. Mishin, I. Shishov, O. Stolyarov, I. Kasatkin, P. Glukhov. *Mater.*, **11**, 100726 (2020).
- [43] Electronic source. Available at:
www.physics.nist.gov/PhysRefData/ASD/lines_form.html